Organic LETTERS

Letter

pubs.acs.org/OrgLett

# Tabercorymines A and B, Two Vobasinyl–Ibogan-Type Bisindole Alkaloids from *Tabernaemontana corymbosa*

Yu-Xi Yuan,[†,‡] Yu Zhang,*[,†] Ling-Li Guo,[†] Yue-Hu Wang,[§] Masuo Goto,[⊥] Susan L. Morris-Natschke,[⊥] Kuo-Hsiung Lee,*[,⊥,∥] and Xiao-Jiang Hao*[,†]

[†]State Key Laboratory of Phytochemistry and Plant Resources in West China and [§]Key Laboratory of Economic Plants and Biotechnology, Kunming Institute of Botany, Chinese Academy of Sciences, Kunming 650201, China

[‡]Yunnan University of Traditional Chinese Medicine, Kunming 650500, China

[⊥]Natural Product Research Laboratories, UNC Eshelman School of Pharmacy, University of North Carolina, Chapel Hill, North Carolina 27599-7568, United States

[∥]Chinese Medicine Research and Development Center, China Medical University and Hospital, 2 Yuh-Der Road, Taichung 40447, Taiwan

Supporting Information

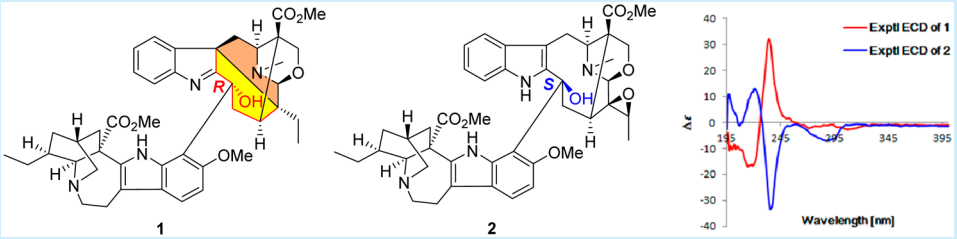


**ABSTRACT:** Tabercorymines A (**1**) and B (**2**), two new vobasinyl–ibogan-type bisindole alkaloids with an unprecedented skeleton, were isolated from *Tabernaemontana corymbosa*. Their structures were established by a combination of spectroscopic data, chemical transformation, single-crystal X-ray diffraction, and ECD calculation. Compound **1** represents a novel bisindole alkaloid, characterized by a caged heteropentacyclic ring system incorporating an unprecedented C-7/C-20 bond in the vobasinyl unit. Alkaloids **1** and **2** showed potent antiproliferative activity against several human cancer cell lines, including vincristine-resistant KB.

Monoterpenoid indole alkaloids (MIAs) are characteristic secondary metabolites found mainly in the plants of the Apocynaceae, Loganiaceae, and Rubiaceae families. With diverse structures and intriguing biological activities, they have long been attractive and challenging subjects of natural products and synthetic chemistry.[1] Among the MIAs, the dimeric vincristine and its derivatives are quite outstanding due to their famous anticancer activity.[2] The shrubs or small trees in the genus *Tabernaemontana* (Apocynaceae) are distributed mainly in Asia, Africa, America, and the Pacific Islands, with five species found in the southern area of China.[3] Previous studies demonstrated that the genus is rich in MIAs and their dimers, and new MIAs characterized by structural complexity and significant anticancer activity have been isolated and identified in recent years.[4] In our further search for structurally unique and bioactive MIAs,[5] two new bisindole alkaloids, tabercorymines A (**1**) and B (**2**), and a biogenetically related alkaloid, tabernaricatine A,[6] were isolated from the twigs and leaves of *T. corymbosa*. **1** represents a new class of vobasinyl–ibogan-type bisindole alkaloids characterized by a caged heteropentacyclic ring system due to the unique formation of C-7/C-20 bond in the vobasinyl unit (Figure 1). This paper describes the isolation, structure elucidation, and antiproliferative properties of the new alkaloids, as well as a plausible biosynthetic pathway for their generation.

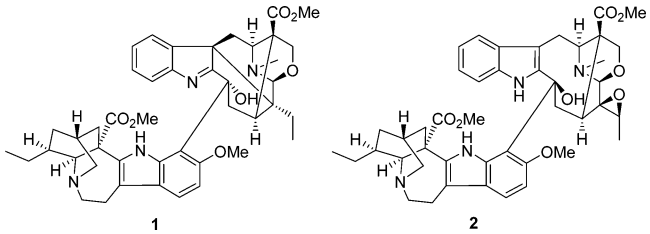


**Figure 1.** Structures of tabercorymines A (**1**) and B (**2**).

**1** was obtained as a white amorphous powder. Its molecular formula was determined as $C_{44}H_{52}N_4O_7$ by HRESIMS at $m/z$ 749.3922 $[M + H]^+$ (calcd749.3909) with 21 indices of hydrogen deficiency. IR bands at 3444 and 1729 $cm^{-1}$ suggested the presence of amino or hydroxyl groups and ester carbonyl functionalities, respectively. UV absorptions at $\lambda_{max}$ (log $\varepsilon$) 278 (4.25), 227 (4.88), 207 (4.72) nm were typical of indole

**Received:** August 8, 2017
**Published:** September 6, 2017





DOI: 10.1021/acs.orglett.7b02445
*Org. Lett.* 2017, 19, 4964–4967

**Table 1. $^1$H and $^{13}$C NMR Data of Tabercorymine A (1) in Acetone-$d_6$ ($\delta$ in ppm and $J$ in Hz)**

| unit A | | | unit B | | |
|---|---|---|---|---|---|
| no. | $\delta_H$ [a] | $\delta_C$ [b] | no. | $\delta_H$ [a] | $\delta_C$ [b] |
| 2 | | 191.7 | 2′ | | 137.0 |
| 3 | | 74.5 | 3′a | 2.90 [c] | 52.5 |
| 5 | 3.59 (br d, 4.2) | 55.9 | 3′b | 2.83 [c] | |
| 6a | 3.06 (br d, 13.8) | 34.6 | 5′a | 3.35 (ddd, 18.0, 12.0, 6.0) | 54.0 |
| 6b | 2.01 (dd, 13.8, 4.8) | | 5′b | 3.15 [c] | |
| 7 | | 61.2 | 6′a | 3.14 [c] | 22.6 |
| 8 | | 144.8 | 6′b | 2.94 (ddd, 12.0, 6.0, 4.2) | |
| 9 | 7.64 (d, 7.2) | 126.0 | 7′ | | 109.5 |
| 10 | 7.18 (td, 7.2, 1.2) | 126.2 | 8′ | | 126.3 |
| 11 | 7.26 (td, 7.2, 1.2) | 128.2 | 9′ | 7.31 (d, 8.4) | 118.9 |
| 12 | 7.34 (d, 7.2) | 120.5 | 10′ | 6.74 (d, 8.4) | 108.7 |
| 13 | | 156.9 | 11′ | | 151.5 |
| 14a | 2.68 (dd, 15.0, 10.2) | 39.0 | 12′ | | 119.2 |
| 14b | 2.01 (dd, 15.0, 5.4) | | 13′ | | 136.1 |
| 15 | 2.61 (dd, 10.2, 5.4) | 35.3 | 14′ | 1.86 (m) | 28.4 |
| 16 | | 53.5 | 15′a | 1.73 (m) | 33.1 |
| 17a | 3.97 (d, 9.0) | 69.0 | 15′b | 1.09 (m) | |
| 17b | 3.97 (d, 9.0) | | 16′ | | 55.7 |
| 18 | 0.74 (t, 7.2) | 9.2 | 17′a | 2.58 (br d, 13.8) | 36.7 |
| 19a | 1.98 (q, 7.2) | 25.4 | 17′b | 1.96 (br d, 13.8) | |
| 19b | 0.94 (q, 7.2) | | 18′ | 0.89 (t, 7.2) | 11.9 |
| 20 | | 48.6 | 19′a | 1.57 (dq, 21.0, 7.2) | 27.6 |
| 21 | 4.30 (br s) | 91.3 | 19′b | 1.42 (dq, 21.0, 7.2) | |
| $CO_2Me$ | 3.55 (s) | 52.2 | 20′ | 1.37 (m) | 39.7 |
| | | 173.5 | 21′ | 3.54 (br s) | 58.1 |
| | | | NH | 9.38 (br s) | |
| NMe | 2.90 (s) | 39.5 | 11′-OMe | 3.30 (s) | 57.4 |
| 3-OH | 5.06 (s) | | | | |
| | | | $CO_2Me'$ | 3.73 (s) | 52.6 |
| | | | | | 175.6 |

[a]Measured at 600 MHz. [b]Measured at 150 MHz. [c]Overlapped, without designating multiplicity.

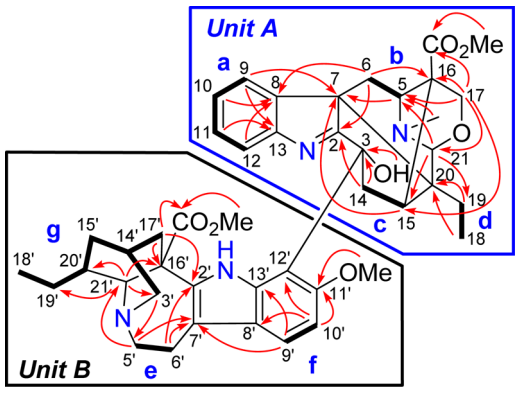


**Figure 2.** $^1$H−$^1$H COSY (—) and selected HMBC (→) correlations of **1**.

**Scheme 1. Preparation of 1a (Dehydrated Derivative of 1)**

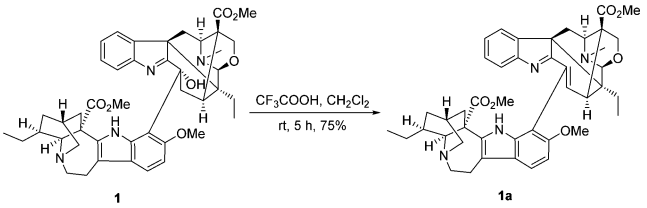


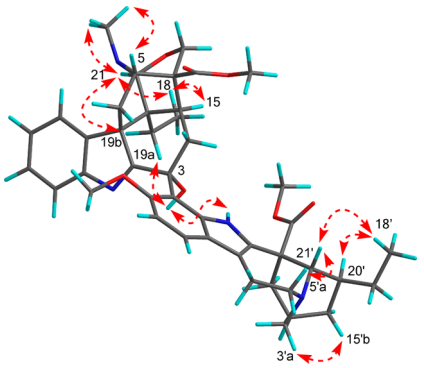


**Figure 3.** ROESY (↔) correlations of **1**.

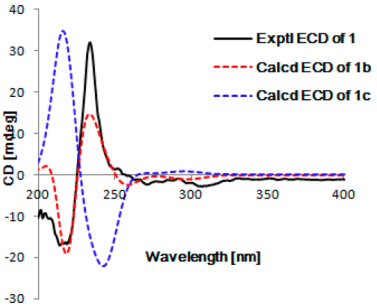


**Figure 4.** Comparison of the experimental ECD and calculated ECD spectra of **1**.

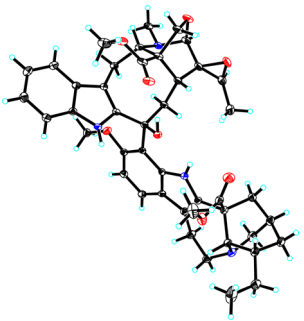

**Figure 5.** X-ray crystal structure of **2**.

chromophores.[7] $^{13}$C NMR and DEPT data (Table 1) suggested that **1** possessed 44 carbon signals, which were classified as six methyls, 10 methylenes, 12 methines, and 16 quaternary carbons. Further analysis of the NMR spectra indicated that **1** was a bisindole alkaloid containing typical ibogan and vobasinyl units.[8] The structures of units A and B and their connectivities were established from 2D NMR analyses (HSQC, $^1$H−$^1$H COSY, and HMBC) (Figure 2).

In unit A, $^1$H−$^1$H COSY correlations of four deshielded protons ($\delta_H$ 7.64 (d, $J$ = 7.2 Hz, H-9), 7.18 (td, $J$ = 7.2, 1.2 Hz, H-10), 7.26 (td, $J$ = 7.2, 1.2 Hz, H-11), and 7.34 (d, $J$ = 7.2 Hz, H-



DOI: 10.1021/acs.orglett.7b02445
Org. Lett. 2017, 19, 4964−4967

**Scheme 2. Hypothetical Biosynthetic Pathway to 1**

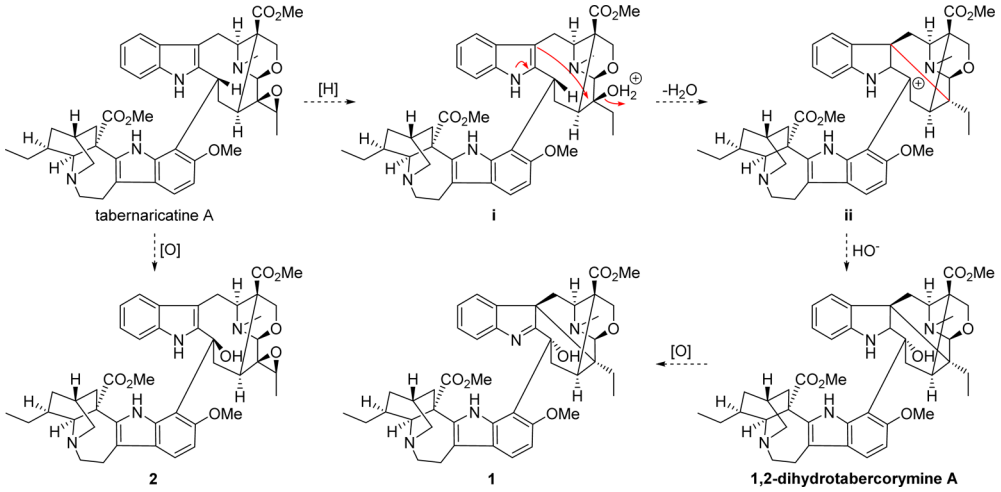


**Table 2. Antiproliferative Activities of 1, 1a, and 2 ($IC_{50}$ in $\mu$M) in Vitro**

| | A-549 | MDA-MB-231 | KB | KB-VIN | MCF-7 |
|---|---|---|---|---|---|
| 1 | 4.8 ± 0.1 | 6.4 ± 0.0 | 9.8 ± 0.2 | 8.9 ± 0.4 | 12.9 ± 0.2 |
| 1a | *a* | *a* | *a* | *a* | *a* |
| 2 | 27.9 ± 2.6 | 20.5 ± 0.2 | 16.7 ± 1.6 | 9.6 ± 0.3 | 23.5 ± 0.1 |
| VIN (nM) | 20.5 ± 1.7 | 32.6 ± 7.6 | 2.6 ± 0.0 | 1700.6 ± 59.7 | 7.2 ± 0.2 |

[a] $IC_{50}$ > 40 $\mu$M.

12) and HMBC correlations of H-6a ($\delta_H$ 3.06 (br d, $J$ = 13.8 Hz)) to C-2 ($\delta_C$ 191.7) suggested the presence of an unsubstituted 3*H*-indole moiety. HMBC correlation of H-5 ($\delta_H$ 3.59 (br d, $J$ = 4.2 Hz)) to C-7 established connectivity between the 3*H*-indole moiety and subunit **b**. The presence of a 3-methyl-1,3-oxazinane ring system was elucidated by HMBC correlations of H-17 ($\delta_H$ 3.97 (d, $J$ = 9.0 Hz)) to C-5 ($\delta_C$ 55.9) and C-21 ($\delta_C$ 91.3) and of H-21 ($\delta_H$ 4.30 (d, $J$ = 1.2 Hz)) and NMe ($\delta_H$ 2.90 (s)) to C-5. HMBC cross-peaks of $CH_3$-18 ($\delta_H$ 0.74 (t, $J$ = 7.2 Hz)) and H-19a ($\delta_H$ 1.98) to C-20 ($\delta_C$ 48.6) and of H-21 to C-15 ($\delta_C$ 35.3) and C-19 ($\delta_C$ 25.4) led to the connections of the 1,3-oxazinane ring to subunits **c** and **d** via C-20. The novel linkage between the two quaternary carbon atoms (C-7 and C-20) was supported by a key HMBC correlation between H-15 ($\delta_H$ 2.61 (dd, $J$ = 10.2, 5.4 Hz)) and C-7. Connection of the 3*H*-indole moiety to subunit **c** via C-3 ($\delta_C$ 74.5) was corroborated by HMBC correlations of H-14a ($\delta_H$ 2.68 (dd, $J$ = 15.0, 10.2 Hz)) to C-2 and C-3 and of OH-3 ($\delta_H$ 5.06 (s)) to C-3. HMBC correlations of H-17 to C-15, C-16 ($\delta_C$ 53.5), and the ester carbonyl ($\delta_C$ 173.5) indicated C-15 and the ester carbonyl were attached to C-16. Finally, the planar structure of unit A was established (Figure 2), with the quaternary carbon atom C-3 as a "loose end" (unassigned substituent).

The chemical shift patterns in unit B were characteristic of those found with ibogan-type alkaloids, further verified by analysis of the HSQC, $^1H-^1H$ COSY, and HMBC spectra (Figure 2). The planar structure of unit B is highly similar to that of isovoacangine,[9] except a $sp^2$ methine signal ($\delta_H$ 6.76 (s); $\delta_C$ 94.2) assigned as C-12 in isovoacangine was replaced by a $sp^2$ quaternary carbon atom ($\delta_C$ 119.2) in unit B of **1**. A key HMBC correlation between H-10′ ($\delta_H$ 6.74 (d, $J$ = 8.4 Hz)) and C-12′ ($\delta_C$ 119.2) confirmed C-12′ as the probable linkage point for units B and A. Because the quaternary carbon atom C-3 in unit A had an unassigned connection, A and B were most likely linked through C-3 and C-12′, respectively.

To confirm the linkage between A and B in **1**, its dehydrated derivative, **1a**, was prepared (Scheme 1). Key HMBC correlation between H-14 ($\delta_H$ 6.65 (d, $J$ = 6.0 Hz)) and C-12′ ($\delta_C$ 109.5) in **1a** (Figure S16) unambiguously established the linkage between C-3 and C-12′ in **1a** and **1**. Thus, the planar structure of **1** was finally established (Figure 2).

The relative configuration of **1** was deduced from the analysis of its ROESY spectra in combination with molecular modeling studies (Figure 3). In A, the ROESY correlations of H-5/N-$CH_3$, N-$CH_3$/H-21, H-21/H-19b, H-21/$CH_3$-18, and $CH_3$-18/H-15 indicated that all of these protons, including $CH_2$-19, were cofacial and arbitrarily assigned as $\alpha$-oriented. Meanwhile, the ROESY correlations of OH-3 with H-19a established the $\alpha$-orientation of OH-3. The ROESY correlations of unit B was identical with those of isovoacangine and coronaridine.[9,10] The relative configuration of **1** was established as 3*R**,5*S**,7*R**,15*S**,16*S**,20*S**,21*S**,14′*R**,16′*S**,20′*S**,21′*S**.

The striking structural difference between **1** and known vobasinyl−ibogan-type bisindole alkaloids is in the vobasinyl unit. Because the absolute configuration of the ibogan unit has been well-demonstrated,[4c,11] the absolute configuration of **1** has two possibilities (3*R*,5*S*,7*R*,15*S*,16*S*,20*S*,21*S*,14′*R*,16′*S*,20′*S*,21′*S*)-**1** (**1b**) and (3*S*,5*R*,7*S*,15*R*,16*R*,20*R*,21*R*,14′*R*,16′*S*,20′*S*,21′*S*)-**1** (**1c**). The absolute configuration of **1** was finally resolved by the calculated results from electronic circular dichroism (ECD) spectra using time-dependent density functional theory performed with Gaussian09.[12] The overall calculated ECD spectra of the **1b** matched well with the experimentally recorded ECD spectra (Figure 4). Therefore, the absolute configuration of **1** could be defined unequivocally as shown in Figure 1.

**2** has the molecular formula $C_{44}H_{52}N_4O_8$ as established by HRESIMS at $m/z$ 765.3849 $[M+H]^+$ (calcd 765.3858), 16 mass units larger than that of tabernaricatine A.[6] The $^1H$ and $^{13}C$ NMR spectra of **2** (Table S1) are strikingly similar to those of



DOI: 10.1021/acs.orglett.7b02445
*Org. Lett.* 2017, 19, 4964−4967

tabernaricatine A, except for the presence of one oxygenated quaternary carbon resonance at $\delta_C$ 76.1 in **2**; namely, **2** was a hydrated derivative of tabernaricatine A. The HMBC correlation of H-14b ($\delta_H$ 2.48 (dd, $J$ = 15.0, 3.5 Hz)) to C-3 ($\delta_C$ 76.1) led to the assignment of the oxygenated quaternary carbon as C-3. The planar structure of **2** was constructed as shown in Figure S24, which was further confirmed by 2D NMR (HSQC, $^1$H−$^1$H COSY, and HMBC) spectra. The absolute configuration of **2** was finally established by X-ray diffraction analysis with Flack parameter 0.11(4) and Hooft parameter 0.10(4) for 2937 Bijvoet pairs (Figure 5).[13,14]

Establishment of the absolute configuration of **2** also indicated that the absolute configurations of C-16 and C-14′ in tabernaricatine A should be 16*S*,14′*R* rather than 16*R*,14′*S*. Note that the ECD curves of **1** and **2** were affected mainly by the absolute configuration of C-3.

The unusual caged heteropentacyclic ring system in **1** resulted from the formation of the C-7/C-20 bond. Biogenetically, **1** might be produced from tabernaricatine A through an intramolecular nucleophilic addition reaction as a key step. Alkaloid **2** could be obtained from tabernaricatine A by oxidation with mono-oxygenase (Scheme 2). The discovery of new alkaloids **1** and **2** might shed light on the total biosynthesis of interesting polycyclic systems of this alkaloid type and contribute to our knowledge of these complex and fascinating alkaloids.

**1** and **2**, as well as **1a**, were evaluated for antiproliferative activity against A-549, MDA-MB-231, KB, KB-VIN, and MCF-7 human cancer cell lines using the SRB method with vincristine (VIN) as the positive control.[15,16] **1** and **2** exhibited significant and comparable antiproliferative activity against multi-drug-resistant KB subline KB-VIN cell line (Table 2), whereas **1** was more potent than **2** against the other cell lines. In contrast, **1a** was inactive against the above human cancer cell lines ($IC_{50}$ > 40 $\mu$M). Note that the hydroxylated stereocenter at C-3 appears to be a critical factor contributing to the antiproliferative activity of such alkaloids. The effect of **1** on cell cycle was evaluated by flow cytometry against MDA-MB-231 triple-negative breast cancer (Figure S29A). Immunostaining of tubulin in the cells treated with **1** showed no significant effect on microtubule morphology (Figure S29B).[15,16] The results demonstrated that **1** showed potential to induce cell cycle arrest at G2/M at a higher concentration without interfering with microtubule formation. Further mechanistic studies are still underway, and the results will be reported in due course.

## ■ ASSOCIATED CONTENT

### Supporting Information

The Supporting Information is available free of charge on the ACS Publications website at DOI: 10.1021/acs.orglett.7b02445.

MS, HRESIMS, IR, UV, ECD, NMR spectra, isolation procedures, computational methods, bioactivity assay (PDF)

X-ray data for **2** (CIF)

## ■ AUTHOR INFORMATION


### Corresponding Authors

*E-mail: zhangyu@mail.kib.ac.cn.
*E-mail: khlee@unc.edu.
*E-mail: haoxj@mail.kib.ac.cn.

### ORCID

Kuo-Hsiung Lee: 0000-0002-6562-0070

Xiao-Jiang Hao: 0000-0001-9496-2152


### Notes

The authors declare no competing financial interest.

## ■ ACKNOWLEDGMENTS

This research was financially supported by the National Natural Science Foundation of China (81473122 and 21432010), CAS "Light of West China" Program (to Y.Z.), the Youth Innovation Promotion Association of CAS (2015323), the Young Academic and Technical Leader Raising Foundation of Yunnan Province (to Y.Z.), and State Key Laboratory of Phytochemistry and Plant Resources in West China (P2016-ZZ08). This study was also supported in part by NIH Grant CA177584 from the National Cancer Institute awarded to K.H.L., and the Eshelman Institute for Innovation, Chapel Hill, North Carolina, awarded to M.G.

## ■ REFERENCES


(1) Dewick, P. M. Alkaloids. In *Medicinal Natural Products: A Biosynthetic Approach*; John Wiley & Sons Ltd.: Chichester, 2009; pp 369−380.

(2) Newman, D. J.; Cragg, G. M. *J. Nat. Prod.* **2016**, *79*, 629−661.

(3) Li, P. T.; Leeuwenberg, A. J. M.; Middleton, D. J. *Flora of China*; Science Press: Beijing, 1995; Vol. *16*, pp 152−153.

(4) (a) Hirasawa, Y.; Miyama, S.; Hosoya, T.; Koyama, K.; Rahman, A.; Kusumawati, I.; Zaini, N. C.; Morita, H. *Org. Lett.* **2009**, *11*, 5718−5721. (b) Ma, K.; Wang, J. S.; Luo, J.; Yang, M. H.; Kong, L. Y. *J. Nat. Prod.* **2014**, *77*, 1156−1163. (c) Lim, K. H.; Raja, V. J.; Bradshaw, T. D.; Lim, S. H.; Low, Y. Y.; Kam, T. S. *J. Nat. Prod.* **2015**, *78*, 1129−1138. (d) Sim, D. S. Y.; Teoh, W. Y.; Sim, K. S.; Lim, S. H.; Thomas, N. F.; Low, Y. Y.; Kam, T. S. *J. Nat. Prod.* **2016**, *79*, 1048−1055.

(5) (a) Zhang, Y.; Guo, L. L.; Yang, G. M.; Guo, F.; Di, Y. T.; Li, S. L.; Chen, D. Z.; Hao, X. J. *Fitoterapia* **2015**, *100*, 150−155. (b) Fu, Y. H.; Di, Y. T.; He, H. P.; Li, S. L.; Zhang, Y.; Hao, X. J. *J. Nat. Prod.* **2014**, *77*, 57−62. (c) Guo, L. L.; He, H. P.; Di, Y. T.; Li, S. F.; Cheng, Y. Y.; Yang, W.; Li, Y.; Yu, J. P.; Zhang, Y.; Hao, X. J. *Phytochemistry* **2012**, *74*, 140−145. (d) Wang, L.; He, H. P.; Di, Y. T.; Zhang, Y.; Hao, X. J. *Tetrahedron Lett.* **2012**, *53*, 1576−1578.

(6) Bao, M. F.; Yan, J. M.; Cheng, G. G.; Li, X. Y.; Liu, Y. P.; Li, Y.; Cai, X. H.; Luo, X. D. *J. Nat. Prod.* **2013**, *76*, 1406−1412.

(7) Sheludko, Y.; Gerasimenko, I.; Kolshorn, H.; Stockigt, J. *J. Nat. Prod.* **2002**, *65*, 1006−1010.

(8) Kam, T. S.; Sim, K. M.; Pang, H. S. *J. Nat. Prod.* **2003**, *66*, 11−16.

(9) Agwada, V. C.; Morita, Y.; Renner, U.; Hesse, M.; Schmid, H. *Helv. Chim. Acta* **1975**, *58*, 1001−1016.

(10) Okuyama, E.; Gao, L. H.; Yamazaki, M. *Chem. Pharm. Bull.* **1992**, *40*, 2075−2079.

(11) Zhang, D. B.; Yu, D. G.; Sun, M.; Zhu, X. X.; Yao, X. J.; Zhou, S. Y.; Chen, J. J.; Gao, K. *J. Nat. Prod.* **2015**, *78*, 1253−1261.

(12) (a) Frisch, M. J.; et al. *Gaussian 09*, revision C.01; Gaussian, Inc.: Wallingford, CT, 2010 (see Supporting Information for full reference). (b) Ishida, K.; Maksimenka, K.; Fritzsche, K.; Scherlach, K.; Bringmann, G.; Hertweck, C. *J. Am. Chem. Soc.* **2006**, *128*, 14619−14624.

(13) Flack, H. D.; Bernardinelli, G. *Chirality* **2008**, *20*, 681−690.

(14) Hooft, R. W. W.; Straver, L. H.; Spek, A. L. *J. Appl. Crystallogr.* **2008**, *41*, 96−103.

(15) Nakagawa-Goto, K.; Taniguchi, Y.; Watanabe, Y.; Oda, A.; Ohkoshi, E.; Hamel, E.; Lee, K. H.; Goto, M. *Bioorg. Med. Chem.* **2016**, *24*, 6048−6057.

(16) Nakagawa-Goto, K.; Oda, A.; Hamel, E.; Ohkoshi, E.; Lee, K. H.; Goto, M. *J. Med. Chem.* **2015**, *58*, 2378−2389.




DOI: 10.1021/acs.orglett.7b02445
*Org. Lett.* 2017, 19, 4964−4967